Journal of Agrometeorology

ISSN : 0972-1665 (print), 2583-2980 (online)
Vol. No. 27 (1) : 12-21 (March - 2025)
https://doi.org/10.54386/jam.v27i1.2846
https://journal.agrimetassociation.org/index.php/jam

Research Paper

Evaluation of NOAH-LSM model over Pune and Ranchi in different seasons

JOSNA MURMU[1], LATHA RADHADEVI[2*], MANOJ KUMAR[1] and MURTHY S BANDARU[2]

[1]*Central University of Jharkhand, Ranchi*
[2]*Indian Institute of Tropical Meteorology, NCL Post, Pune-411008*
**Corresponding author email: latha@tropmet.res.in*

ABSTRACT

Soil moisture (SM) and atmospheric parameters determine the surface energy partition, which impacts near-surface air temperature and moisture. Two locations, Pune and Ranchi, with different soil moisture (SM at Pune with clay soil is higher than that at Ranchi with loam soil), are chosen to evaluate the NOAH land surface model (NCEP, OSU-version 2.7.1) for winter, pre-monsoon and post-monsoon seasons. We have used the estimated surface fluxes by eddy covariance technique for the model validation. Agreement is better between the model and observations of net shortwave radiation for dry soil than that for wet soil, such a feature caused by surface albedo mismatch. Model validation of sensible (H) and latent (LE) heat fluxes at Pune indicate better agreement overall for winter (Jan; R^2 and RMSE for H, 0.72, 34) and post-monsoon (Nov; 0.67, 56) compared to summer, (May; 0.55, 70). Similar is the case at Ranchi, with R^2 and RMSE for winter and post-monsoon (January: 0.8, 24 & November: 0.9, 14) better and lower for summer (May: 0.7, 65). Bowen ratio (Model) for wet soil (0.45) is lower than that for dry soil (0.6). The model underestimates ground heat flux for wet soil and overestimates for dry soil due to soil thermal and hydraulic conductivity uncertainty. Further improvement of parameterization schemes in the land surface models would help better understand soil hydrology and boundary layer development.

Keywords: Land surface model; Bowen ratio, Sensible heat flux; Latent heat flux; Soil heat flux; Radiation

Surface energy fluxes, driving atmospheric convection and precipitation, mainly depend on net radiation and soil moisture. Partition of net radiation into sensible, latent and ground heat fluxes varies spatially and temporally due to land-use patterns and soil moisture variability. Soil moisture (dry or wet soil) modifies surface albedo, determining how much incident radiation gets reflected, influencing net radiation. Soil heat flux varies with soil moisture, and a fraction of net radiation goes into soil as soil heat flux; remaining available energy at the surface partitions into sensible and latent heat fluxes. Surface energy budget and its seasonal variation using observations (Murthy *et al.,* 2001; Patil *et al.,* 2001; Kumar *et al.,* 2007; Ghosh *et al.,* 2023) and remote sensing (Danodia *et al.,* 2024 a, b) have been reported by several studies. Evaporation (latent heat flux) consists of evaporation from the soil, transpiration by vegetation and canopy water evaporation (Liang and Guo, 2003; Han *et al.,* 2008; Rosero *et al.,* 2010). Canopy water is free water settled on the canopy due to precipitation or dew fall and depends on plant type, actual water content and shading factor (Pan and Mahrt, 1987). Evaporation from soil is linearly dependent on soil moisture if soil moisture is less than the threshold/critical value (soil moisture control regime). This threshold value lies between the field capacity and the wilting point and varies according to soil type. Soil evaporation becomes insensitive to soil moisture when its value exceeds the critical/threshold value. Its variation is further controlled by radiation and relative humidity/saturated water vapour deficit/atmospheric demand. The soil moisture threshold, at which the evaporation regime shifts from soil to the atmosphere, has a large spatial variability (Haghighi *et al.,* 2018). Dry soil causes relatively more sensible heat flux, while wet soil results in more latent heat flux; thus, soil moisture regulates energy partition at the land surface and influences near-surface climate. Land-atmosphere interactions are complex, involving energy exchange processes for various land-use patterns like wetlands, irrigated crops, plant canopies, lakes, and so on (Fisher and Koven, 2020), influencing roughness length for momentum, soil moisture and partitioning of net radiation into surface fluxes. Sensible and latent heat fluxes determine vertical

Article info - DOI: *https://doi.org/10.54386/jam.v27i1.2846*
Received: 13 December 2024; Accepted: 28 January 2025 ; Published online : 1 March 2025

temperature and moisture profiles, and their gradients determine the degree of vertical static instability, convection, and precipitation. Precipitation neutralizes instability, bringing the atmosphere back to stable conditions with clear skies, which increases incident solar radiation at the surface and causes convective cloud development again (Rajagopal *et al.,* 2001; Murthy *et al.,* 2004).

NOAH-LSM is either used offline with given atmospheric forcing (Bowling *et al.,* 2003), two-dimensional horizontal land surface domains and three-dimensional fully coupled mesoscale models (Marshall *et al.,* 2003). The soil thermal conductivity is determined by the porosity, type of texture, and soil moisture content (Peters-Lidard *et al.,* 1997) in the case of soil moisture-dependent soil thermal conductivity.

Land surface heterogeneity can be seen over the Indian sub-continent in the tropics because soil properties change at a spatial scale of around 50 km (Singh *et al.,* 2005). Typically, soils are not homogeneous in composition; hence, soil properties have large standard deviations. Heat and moisture transport within the soil is simulated using heat and moisture diffusion equations that use thermal and hydraulic conductivity, which are parameterized in terms of soil moisture content and an empirical exponent coefficient. Thermal and hydraulic conductivity are very sensitive to the values of the empirical coefficient. They change by two orders of magnitude if the coefficient changes by one standard deviation (Holtslag and Ek, 2005). So, it becomes essential to study the performance of LSMs for different regions under different meteorological and soil conditions. Various land surface models have been used to study the role of land surface processes at the regional scale (Maity *et al.,* 2017) and the Indian subcontinent scale (Nair and Indu, 2017; Panda and Sharan, 2012). Very few studies have used observed atmospheric and surface forcing in a column model to understand atmosphere-soil-vegetation interactions (Parasnis *et al.,* 2001; Murthy *et al.,* 2004). NOAH-LSM simulations are sparse for the Indian region (Chang *et al.,* 2009), specifically over the Chota-Nagpur plateau.

The study's objective is to evaluate the performance of NOAH-LSM in one-dimensional mode by comparing the simulated heat fluxes with the observed fluxes at two locations with different soil moisture regimes.

MATERIAL AND METHODS

Two locations were selected, one in the Chota-Nagapur plateau (Ranchi, Lat 23.3°N, Lon 85.3°E, 609 m AMSL) and the other in the Deccan plateau (Pune, Lat 18.5°N, Lon 73.8°E, 550 m AMSL) for the evaluation of LSM against in-situ observations. The Chota-Nagpur Plateau, located in eastern India, lies entirely in a humid subtropical monsoon area with hot summers and cold winters. The climate ranges from dry semi-humid to humid semi-arid types. The Deccan plateau has a semi-arid climate in the north with black soil and receives most of its rainfall during the monsoon season. Monthly-mean temperature (T) and relative humidity (RH) in Pune have a range of 26.8^0 C - 29.4^0 C and 42.8% - 85.1% respectively. The same for Ranchi is 14.4^0 C - 29.3^0 C and 28.0% - 64.8% respectively. Surface energy fluxes (Radiation, Sensible and Latent heat), estimated by eddy covariance method using sonic anemometer (Gill and Campbell make) and open-path gas analyzer (Vaisala, LI-7500 at Pune only) at 10 Hz frequency, at Pune and Ranchi (LI-7500 not available here) were used for validation of NOAH-LSM. Observed diurnal fluxes on three continuous clear sky days were chosen for each season (winter, summer and post-monsoon) in Pune and Ranchi for model validation. For Pune, shortwave radiation (SW), sensible heat flux (SHF), soil heat flux (GHF) and latent heat flux (LE) on January 1, 2, 3; May 3, 4, 5 and November 1, 3, 4 were chosen. For Ranchi, SW, SHF, and GHF on January 8, 9, 10; May 1, 2 and November 10, 11, 12 were chosen. Model simulated surface fluxes were used to determine the 'Bowen Ratio' and its temporal variation at both sites. Sensible heat fraction, the ratio of sensible heat flux to net shortwave radiation, are presented in terms of its variation with soil moisture. Other instrument details installed on micro-meteorological towers are given in supplementary material (Table ST1).

In this study, a one-dimensional (column) ABL model (Oregon State University 1-D Coupled Atmospheric Plant Soil (OSU 1-D CAPS) model (Chang *et al.,* 1999), later developed to NOAH-LSM) which has a land-surface scheme that interacts with the ABL is used (Murthy *et al.,* 2004). The model simulates interactions between the atmosphere, soil, and surface (with vegetation). It has three components coupled to each other: the atmospheric boundary layer model, the two-layer soil model and the plant canopy model. Total evaporation is computed as the sum of direct evaporation from the soil, transpiration by vegetation and evaporation of intercepted canopy water from precipitation. Transpiration is formulated in terms of vegetation density, plant resistance and soil moisture. The diffusive equations for water vapor and temperature transport in the soil are used to determine soil moisture and soil temperature by specifying the soil type's wilting point and field capacity. The soil model consists of a top layer of 5 cm thick and a lower layer of 95 cm thick, for which observed soil temperature and moisture values are specified for initializing the model. The atmospheric boundary layer model has 100 m resolution up to 2 km and then 200 m above that. The model time step is 180 sec, and it is initialized at 0 GMT (0530 am IST) and runs for 24 hours. More model details are available elsewhere (Holtslag and Ek, 1996).

This model simulates soil moisture, soil temperature, skin temperature, and the energy flux and water flux terms of the surface energy balance. Profiles of wind (3 components), temperature and water vapour mixing ratio are taken from reanalysis data of the National Centre for Medium-Range Weather Forecasting (NCMRWF). In-situ measurements of soil temperature and soil moisture at two levels are used in the control file. Details of other input parameters are given in Table ST2. Simulations for four months/seasons (January, May and November falling in winter, pre and post-monsoon, respectively) are performed and compared with observed fluxes.

RESULTS AND DISCUSSION

Diurnal variation of radiation, sensible and soil heat fluxes simulated by the model for three days in each season are compared with those observed at Pune and Ranchi. Surface atmospheric pressure, surface albedo, roughness length for momentum and heat, soil temperature and soil moisture at two levels and vertical profile

Table 1: Statistical metrics for model performance of energy fluxes at Pune and Ranchi

Season/Month	R^2				RMSE (W m^{-2})			
	SW	SHF	GHF	LE	SW	SHF	GHF	LE
Pune								
Winter, Jan	0.89	0.72	0.36	0.57	64.57	34.80	15.93	74.93
Summer, May	0.87	0.55	0.22	0.48	94.53	70.98	22.31	114.92
Monsoon, Aug	0.77	0.31	0.32	0.23	177.03	56.35	30.67	62.02
Post-monsoon, Nov	0.86	0.67	0.38	0.72	89.00	56.40	47.33	62.02
Ranchi								
Winter, Jan	0.95	0.8	0.5	na	47.17	24.4	34.1	na
Pre-Summer, Mar	0.95	0.8	0.6	na	66.46	20.3	36.2	na
Summer, May	0.85	0.7	0.7	na	109.79	65.4	38.9	na
Post- Monsoon, Nov	0.90	0.9	0.7	na	69.73	14.31	33.5	na

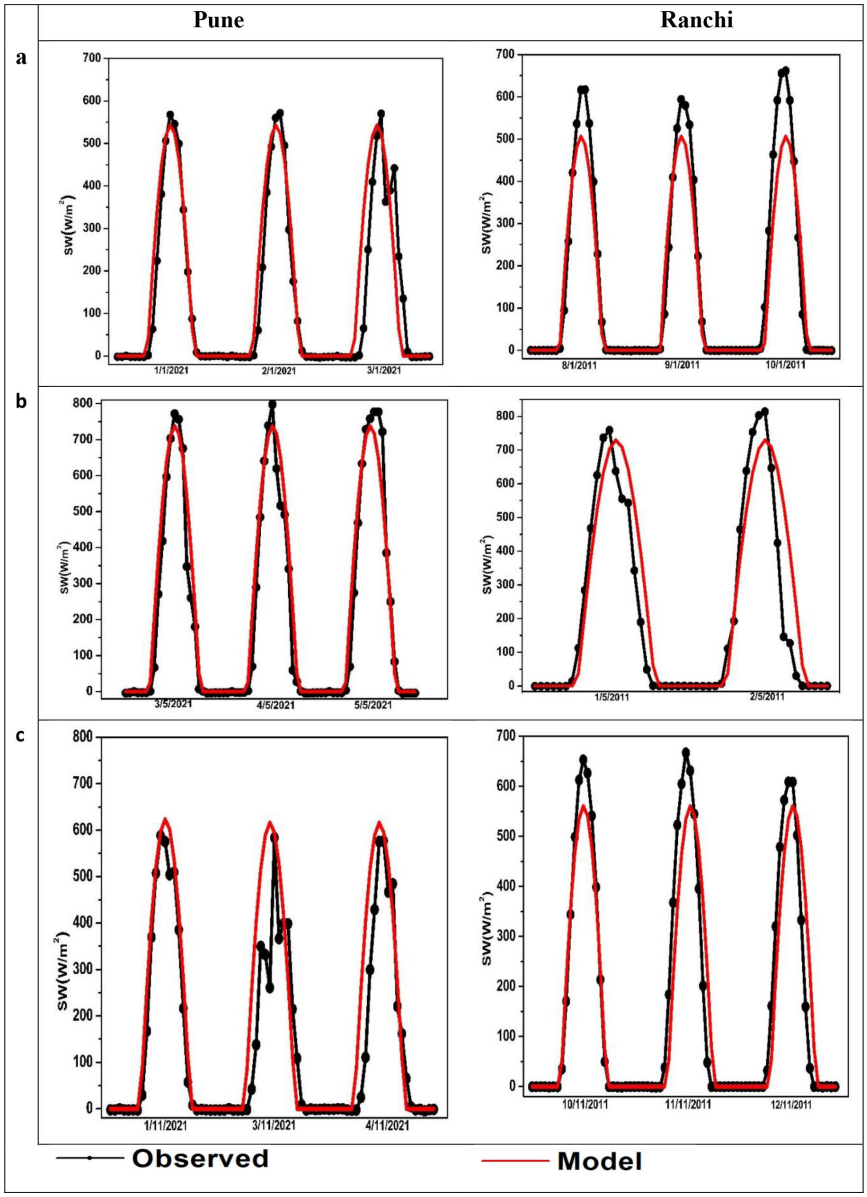

Fig. 1: Diurnal variation of net shortwave radiation (SW) at Pune and Ranchi in a) winter (Jan), b) Summer (May) and c) post-monsoon (Nov)

of wind components (u, v and w), air temperature and water vapour mixing ratio in the atmospheric boundary layer at 00 GMT (0530 h IST) are used for initialization of the model. The model is run for 24 hours.

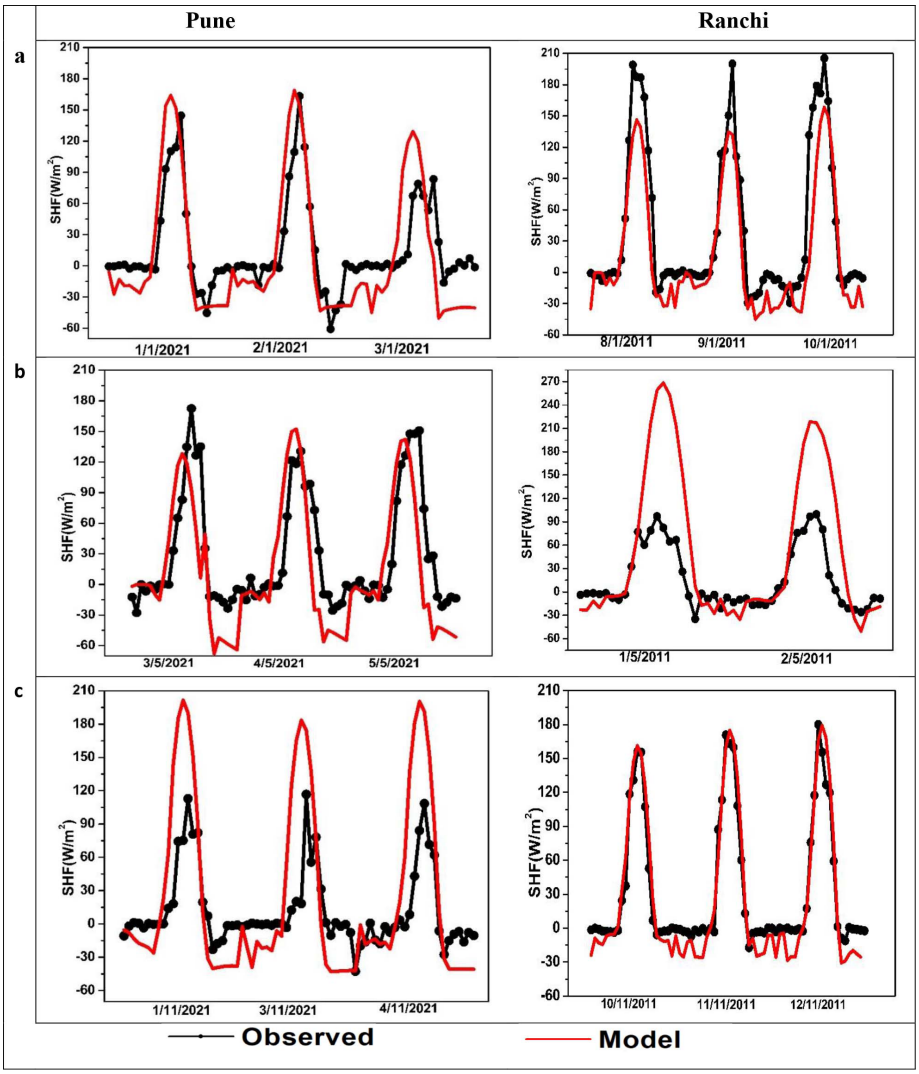

Fig. 2: Diurnal variation of sensible heat flux (SHF) at Pune and Ranchi in a) winter (Jan), b) Summer (May) and c) post-monsoon (Nov)

Net shortwave radiation and sensible heat flux

Fig. 1 illustrates the diurnal variation of net shortwave radiation (SW) at Pune and Ranchi in winter (Fig.1a), summer (Fig.1b) and post-monsoon (Fig.1c). Fig. 2 illustrates the diurnal variation of sensible heat flux (SHF) at Pune and Ranchi in winter (Fig.2a), summer (Fig.2b) and post-monsoon (Fig.2c). Model simulation is reasonably good, though there is an underestimation of radiation at noon by 100 Wm^{-2} at Ranchi in May (Fig.1b) and November (Fig.1c). SHF is overestimated during daytime in Pune, while in Ranchi, it is underestimated (Fig.2). Observations indicate little negative SHF during the night, while the model shows larger negative SHF at Pune as well as Ranchi. More negative SHF during the night in the model indicates relatively more surface cooling, leading to a strong, stable layer. It could be attributed to less cloud cover or more moisture in the model simulation. In Ranchi, the underestimation of SHF in winter (Fig.2a) appears to be due to underestimation of SW. However, the model overestimated SHF in the summer (May) (Fig.2b) despite a reasonably good agreement with the observed SW (Fig.1b). This mismatch appears to be due to the model's arid soil (little soil moisture) compared to the actual soil moisture, which points to the significant role of soil moisture in surface energy partition.

In summer (May), as shown in Fig. 1b, SW simulation looks reasonable (fluctuations in observed SW indicate the presence of clouds), while SHF (Fig.2b) depicts significant overestimation by the model. In post-monsoon (November), the model overestimates SW (Fig.1c) and SHF at Pune (Fig. 2c) and underestimates SW at Pune (Fig.1c). At Ranchi, SHF is well simulated during the day (Fig.2a,b,c) but not at night. The model has negative SHF during the night in all seasons, while observations depict almost negligible SHF.

Heat and water transport in the soil depends on hydraulic conductivity, soil water diffusivity and thermal conductivity, which are parameterized in terms of volumetric soil moisture (and its saturated value) and empirical coefficient, which varies with soil type, soil texture and its heterogeneity (Clapp and Hornberger, 1978). These empirical formulae are valid for homogeneous soil, but the parameters have a large standard deviation for a typical heterogeneous soil.

Simulation of ground heat flux (GHF) and its comparison

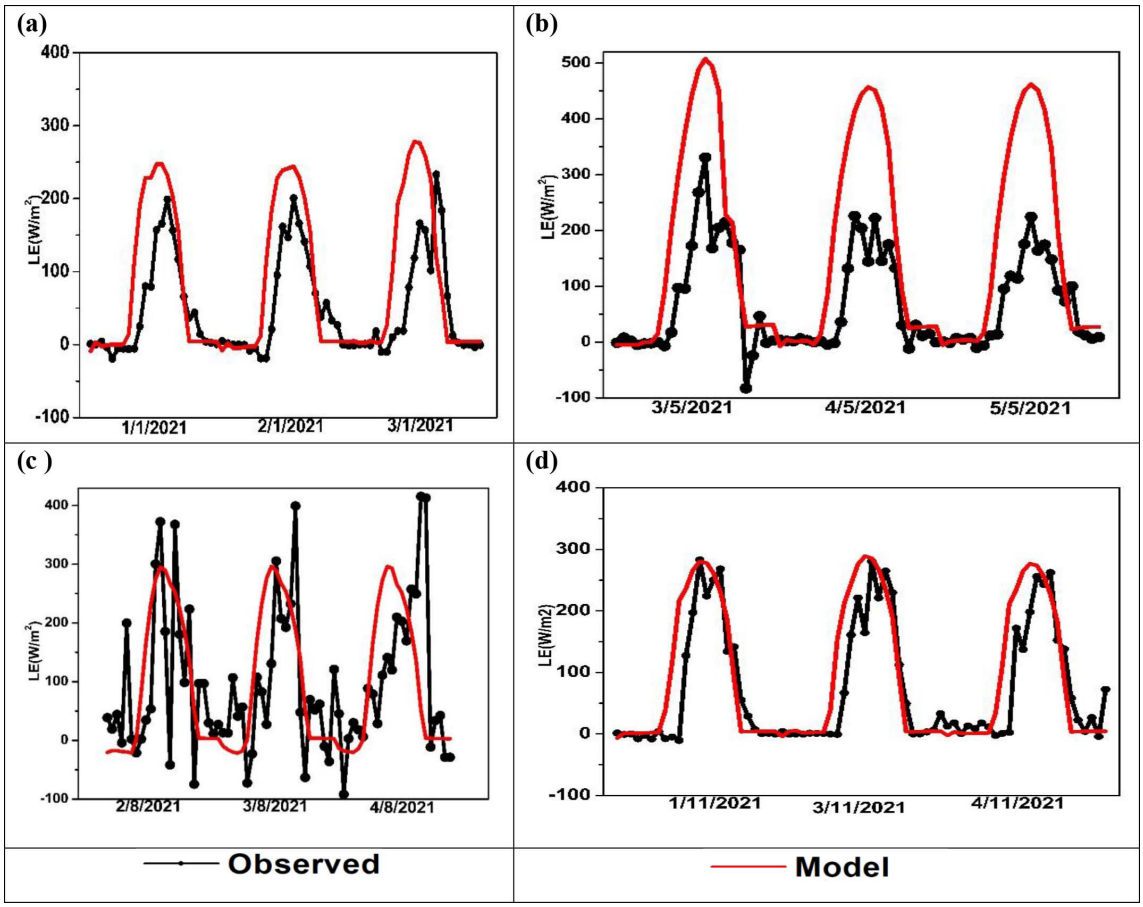

Fig. 3: Diurnal variation of LE by the model and observations for January (a), May (b), August (c) and November (d) at Pune

with observations is shown in Fig.S1 for Jan, May and November, indicates large deviations that could be attributed to uncertainty in soil properties like thermal and hydraulic conductivity of soil, which is a function of highly variable soil moisture in space and time. Thermal properties of soil, like thermal conductivity and diffusivity of the soil, depend on soil type, texture, organic matter content, mineral content, composition (Zhao *et al.,* 2019) and soil moisture (Wang *et al*., 2010). The observed GHF in winter and summer at Ranchi is higher than that at Pune (Fig.S1), indicating that sufficient soil moisture is available at Ranchi to transport heat from the surface into the soil. It implies that the satellite-derived soil moisture at Ranchi is underestimated. The large difference between the modelled and observed GHF could be due to a mismatch of the empirical coefficient.

Simulation of latent heat flux (LE) by the model is compared with observed LE at Pune for Jan, May, Aug and Nov, as illustrated in Fig.3. Simulated values are reasonably in agreement in November. However, in January and May, they are overestimated, although the diurnal pattern is reasonably simulated. The fluctuations in the observed diurnal variation of LE could be attributed to passing cloud patches, soil moisture variations in the topsoil layer and wind speed variation. Since this is a column model, horizontal dynamics like advection and circulations are not accounted.

Statistical metrics evaluating the model performance are given in Table 1 for Pune and Ranchi. Only the common months (Jan, May and Nov) for both places are illustrated for comparison purposes (Fig.1 and Fig.2); for metrics, August is included only for Pune and March for Ranchi.

The model metrics for Pune (Table 1) show the range of correlation (R^2) for SW (0.77-0.89), SHF (0.31-0.72), GHF (0.22-0.38), and LE (0.23-0.72). Bias/RMSE is minimum in winter (Jan) for SW (64 Wm^{-2}), for SHF (34 Wm^{-2}) and GHF (15 Wm^{-2}) and LE in August, November (62 Wm^{-2}). The model metrics for Ranchi (Table 1) show reasonable correlation (R^2) for SW (0.85-0.95), SHF (0.7-0.9) and GHF (0.5-0.7). Bias is minimum in winter for SW (47 Wm^{-2}), for SHF in pre-summer, March (20 Wm^{-2}) and for GHF in post-monsoon, November (33 Wm^{-2}).

Overall, at Pune, the model has shown better performance in winter (Jan) in terms of metrics for energy fluxes (SW, SHF and GHF), while for LE minimum bias and maximum R^2 are in Post-monsoon, Nov. For Ranchi, the model shows maximum bias/RMSE in May for SW, SHF and GHF. Relatively fair-weather conditions prevail in winter and post-monsoon, which helps better represent land-atmosphere interactions, thus resulting in a better agreement between model and observations. During summer/pre-summer (summer changeover) and monsoon, synoptic disturbances modify local weather, leading to uncertainty in land-surface parameterization schemes and simulation (Zhu and Lettenmaier, 2007).

Table 2: Monthly-mean sensible heat fraction (SHF/SW), soil moisture (SM), temperature (T) and relative humidity (RH) in Pune and Ranchi

	Pune					Ranchi			
Month	SHF/SW	SM	T	RH	Month	SHF/SW	SM	T	RH
Jan	0.162	0.196	27.8	49.0	Jan	0.28	0.17	14.5	62.8
May	0.178	0.262	33.1	42.8	Mar	0.20	0.12	26.2	28.0
Aug	0.138	0.441	26.8	71.3	May	0.11	0.17	29.3	43.8
Nov	0.148	0.200	29.4	85.2	Nov	0.23	0.22	19.7	64.8

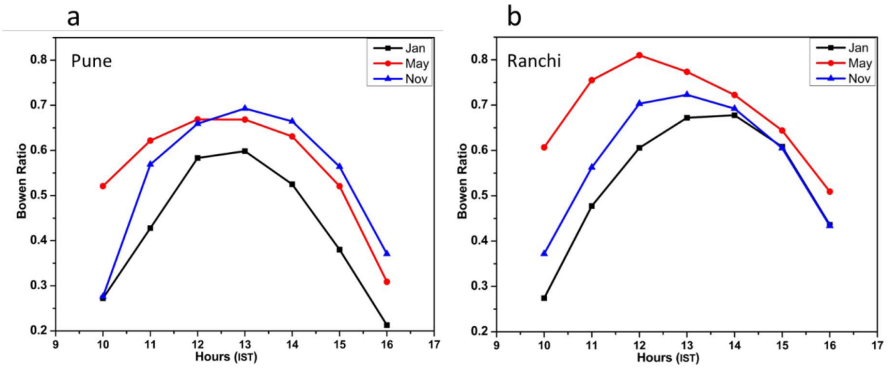

Fig. 4: Model simulated Bowen ratio (B=SHF/LE) diurnal variation (average of 3 days in each month) during 1000 – 1600 h IST in Jan, May and Nov at (a) Pune and (b) Ranchi

Bowen ratio

Surface energy fluxes can be estimated using Bowen ratio (B), net radiation and ground heat flux in the absence of high frequency measurements using expensive instruments like sonic anemometer and gas analyzer. Bowen ratio is the ratio of SHF to LE which can be determined from vertical gradients of air temperature and water vapor mixing ratio in the surface layer. This can be used to distinguish arid (B > 1), and humid (B < 1) regions. Net radiation, Rn, indicates the partition of available energy at the surface into sensible and latent heat/evaporation, which is determined by soil property (soil texture and moisture content). More energy is utilized for soil moisture evaporation in wet soil, while little is used to increase air temperature and vice versa in dry soil. As shown in Fig. 4, the Bowen ratio (SHF/LE) is calculated based on model output for Pune and Ranchi. Its range at Pune (0.2 - 0.7) and Ranchi (0.3 - 0.8) indicate the land surface at Ranchi is drier than at Pune. At Pune, a minimum ratio (0.6 at noon) is observed in Jan, while May and November depict similar variations with a noon peak of 0.7. At Ranchi, the ratio is observed to increase gradually from Jan (0.68) to Nov (0.8) through May (0.72).

Sensible heat fraction

Evaporative fraction (LE/Rn) determines how much of Rn is utilized in the evaporation of soil moisture. As soil dries, evaporation decreases and sensible heat flux increases as soil moisture regulates the partition of Rn into SHF and LE. Observed LE is unavailable at Ranchi. We have used satellite-derived monthly mean soil moisture for both locations. LE/Rn and SHF/Rn vary inversely as a function of soil moisture. In this study, we used SW instead of Rn and presented the monthly mean variation of 'sensible heat fraction' (SHF/SW) with soil moisture (SM), as shown in Table 2. At Ranchi, SM and SHF/SW have a direct linear relationship with a decrease in both SM and the ratio from Jan to May. Evaporative fraction is reported (Jiang *et al.,* 2023, Chen *et al.,* 2024) to be increasing with an increase in soil moisture until SM reaches a threshold beyond which this fraction becomes insensitive to SM but is controlled by atmospheric parameters like radiation, RH (relative humidity) and T (air temperature). Since we used observed SHF (instead of LE), the fraction (SHF/SW) is expected to vary inversely with SM. At Pune, as shown in Table 2, this fraction varies inversely with SM from Jan to Aug, which is obvious. However, at Ranchi, with a decrease in SM, the sensible heat fraction also decreases. This could be owing to the misrepresentation of soil texture or soil conductivity in the case of Ranchi. In contrast, the soil properties of Pune are more or less correctly represented in the model. These results indicate the role of soil moisture in energy partition as inferred from the model performance assessed with seasonal statistical metrics.

CONCLUSIONS

Evaluation of NOAH-LSM for diurnal variation of surface fluxes (radiation, sensible, latent and ground heat fluxes) against observed eddy covariance fluxes for two places with significant soil moisture differences reveals that the model performance is reasonably good for net shortwave radiation, sensible heat flux and latent heat flux in winter and post-monsoon compared to summer and monsoon periods as inferred from statistical metrics (R^2 and RMSE). The simulation of ground heat flux is unsatisfactory and needs fine-tuning of soil parameters (thermal and hydraulic conductivity) that are appropriate for the soil type. Moreover, the satellite-derived SM at Ranchi shows gross underestimation, adding to the deviations. Sensible heat fraction as a function of soil moisture follows the expected inverse variation (Soil control regime) at Pune, unlike that

at Ranchi, where soil moisture has slight seasonal variation. Further improvement of land surface models is required by fine-tuning the empirical coefficients in the thermal and hydraulic conductivity parameterization based on field measurements over various soil types.

ACKNOWLEDGEMENTS

The authors are grateful to Dr T Dharmaraj of IITM for providing data on the meteorological tower observations at Pune. The authors also thank IITM, Pune, BIT, Mesra for their logistic and administrative support.

Funding: This study did not receive any funding.

Author's Declaration**:** Authors declare that the manuscript or its part is not under consideration for publication elsewhere and that it has been approved by all co-authors as well as the competent authorities.

Conflict of Interest**:** The authors declare that there is no conflict of interest.

Data Availability**:** To be provided on request

Author contributions: **Latha. R**: Conceptualization, draft editing, Guidance; **J. Murmu:** Data archival, quality assurance, analysis, Graphs; **Manoj Kumar**: Administrative and moral support; **Murthy S B**.: Draft editing, Guidance

Disclaimer: The contents, opinions and views expressed in the research article published in the Journal of Agrometeorology are the views of the authors and do not necessarily reflect the views of the organizations they belong to.

Publisher's Note: The periodical remains neutral with regard to jurisdictional claims in published maps and institutional affiliations.

REFERENCES

Bowling, L. C., Lettenmaier, D. P., Nijssen, B., Polcher, J., Koster, R. D. and Lohmann, D. (2003). Simulation of high-latitude hydrological processes in the Torne–Kalix basin: PILPS Phase 2 (e): 3: Equivalent model representation and sensitivity experiments. *Global Planet. Change, 38*(1-2): 55-71. https://doi.org/10.1016/S0921-8181(03)00005-5

Chang, S., Hahn, D., Yang, C. H., Norquist, D. and Ek, M. (1999). Validation study of the CAPS model land surface scheme using the 1987 Cabauw/PILPS dataset. *J. Appl. Meteorol.,* 38(4): 405-422. https://doi.org/10.1175/1520-0450(1999)038<0405:VSOTCM>2.0.CO;2

Chang, H. I., Kumar, A., Niyogi, D., Mohanty, U. C., Chen, F. and Dudhia, J. (2009). The role of land surface processes on the mesoscale simulation of the July 26, 2005 heavy rain event over Mumbai, India. *Global Planet. Change,* 67(1-2): 87-103. https://doi.org/10.1016/j.gloplacha.2008.12.005

Chen, X., Pan, Z., Huang, B., Liang, J., Wang, J., Zhang, Z., ... and Huang, Z. (2024). Influence paradigms of soil moisture on land surface energy partitioning under different climatic conditions. *Sci. Total Environ.,* ٩١٦: 170098. https://doi.org/10.1016/j.scitotenv.2024.170098

Clapp, R. B. and Hornberger, G. M. (1978). Empirical equations for some soil hydraulic properties. *Water Resour. Res.,* ٤)١٤): 601-604. https://doi.org/10.1029/WR014i004p00601

Danodia, A., Patel, N., Sehgal, V. and Singh, R. (2024a). Surface energy fluxes and energy balance closure using large aperture scintillometer-based ET station on heterogeneous agricultural landscape in north India. *J. Agrometeorol.,* 26(1): 18-24. https://doi.org/10.54386/jam.v26i1.2447

Danodia, A., Patel, N., Suresh Kumar, Singh, R., Satpathi, A., Chauhan, P. and A. S. Nain. (2024b). Quantifying energy fluxes in Tarai region of India during post-monsoon season: Insights from METRIC model, ET station and remote sensing. *J. Agrometeorol.,* 26(3): 271-278. https://doi.org/10.54386/jam.v26i3.2618

Rajagopal, E. N. (2001). Validation of land surface parameters in NCMRWF model with LASPEX Data set. *J. Agrometeorol.,* 3(1-2), 217-226. https://doi.org/10.54386/jam.v3i1-2.408

Fisher, R. A. and Koven, C. D. (2020). Perspectives on the future of land surface models and the challenges of representing complex terrestrial systems. *J. Advan. Model. Earth Syst.,* 12(4): e2018MS001453. https://doi.org/10.1029/2018MS001453

Ghosh, T., Chakraborty, D., Das, B., Sehgal, V. K., Roy, D., Dhakar, R. and Bag, K. (2023). Estimation of actual evapotranspiration using the simplified-surface energy balance index model on an irrigated agricultural farm. *J. Agrometeorol.,* 25(3): 365-374. https://doi.org/10.54386/jam.v25i3.2254

Haghighi, E., Short Gianotti, D. J., Akbar, R., Salvucci, G. D. and Entekhabi, D. (2018). Soil and atmospheric controls on the land surface energy balance: A generalized framework for distinguishing moisture-limited and energy-limited evaporation regimes. *Water Resour. Res.,* 54(3): 1831-1851. https://doi.org/10.1002/2017WR021729.

Han, Z., Ueda, H. and An, J. (2008). Evaluation and inter comparison of meteorological predictions by five MM5-PBL parameterizations in combination with three land-surface models. *Atmos. Environ.*, 42(2): 233-249. https://doi.org/10.1175/2010JAMC2432.1

Holtslag, A.A.M. and Ek, M. (1996). Simulation of surface fluxes and boundary layer development over the pine forest in HAPEX-MOBILHY. *J. Appl. Meteorol. Climatol.,* 35(2): 202-213. https://doi.org/10.1175/1520-0450(1996)035<0202:SOSFAB>2.0.CO;2

Holtslag, A.A.M. and Ek, M.B. (2005). Atmospheric Boundary

Layer Climates and Interactions with the Land Surface. In M. G. Anderson, & J. J. McDonnell (Eds.), *Encycl. Hydrol. Sci.,* 3: 443-454. https://doi.org/10.1007/s10546-007-9214-5

Jiang, K., Pan, Z., Pan, F., Teuling, A. J., Han, G., An, P., ... and Dong, Z. (2023). Combined influence of soil moisture and atmospheric humidity on land surface temperature under different climatic background. *Isci.,* 26(6): https://doi.org/10.1016/j.isci.2023.106837

Kumar, M., Vyas Pandey and Shekh, A. M. (2007). Surface layer simulation of semi-arid region of India using LASPEX-97 data. *J. Agrometeorol.,* 9(1):115-117. https://doi.org/10.54386/jam.v9i1.1110

Liang, X., and Guo, J. (2003). Inter comparison of land-surface parameterization schemes: sensitivity of surface energy and water fluxes to model parameters. *J. Hydrol.,* 279(1-4), 182-209. https://doi.org/10.1016/S0022-1694(03)00168-9

Maity, S., Satyanarayana, A. N. V., Mandal, M., and Nayak, S. (2017). Performance evaluation of land surface models and cumulus convection schemes in the simulation of Indian summer monsoon using a regional climate model. *Atmos. Res.*, 197: 21-41. https://doi.org/10.1016/j.atmosres.2017.06.023

Marshall, C. H., Crawford, K. C., Mitchell, K. E. and Stensrud, D. J. (2003). The impact of the land surface physics in the operational NCEP Eta model on simulating the diurnal cycle: Evaluation and testing using Oklahoma Mesonet data. *Weather. Forecast.,* 18(5):748-768. https://doi.org/10.1175/1520-0434(2003)018<0748:TIOTLS>2.0.CO;2

Murthy B.S., Dharmaraj T. and Pillai J.S. (2001). Variation of surface energy budget at Anand during different seasons of LASPEX-97. *J. Agrometeorol.,* 3: 67-77. https://doi.org/10.54386/jam.v3i1-2.391

Murthy, B. S., Parasnis, S. S. and Ek, M. (2004). Interactions of the land-surface with the atmospheric boundary layer: case studies from LASPEX. *Curr. Sci.,* 1128-1134. http://www.jstor.org/stable/24109322

Nair, A. S., and Indu, J. (2016). Enhancing Noah land surface model prediction skill over Indian subcontinent by assimilating SMOPS blended soil moisture. *Remote Sens.,* 8(12): 976. https://doi.org/10.3390/rs8120976

Pan, H. L. and Mahrt, L. (1987). Interaction between soil hydrology and boundary-layer development. *Boundary-Layer Meteorol.,* 38:185-202. https://doi.org/10.1007/BF00121563

Panda, J. and Sharan, M. (2012). Influence of land-surface and turbulent parameterization schemes on regional-scale boundary layer characteristics over northern India. *Atmos. Res.,* 112: 89-111. https://doi.org/10.1016/j.atmosres.2012.04.001

Parasnis, S. S., Kulkarni, M. K. and Pillai, J. S. (2001). Simulation of boundary layer parameters using one dimensional atmospheric boundary layer model. *J. Agrometeorol.,* 3(1-2), 261-266. https://doi.org/10.54386/jam.v3i1-2.411

Patil M.N., Murthy B.S. and Parasnis S.S. (2001). Characteristics of momentum and sensible heat flux during the monsoon conditions over LASPEX region. *J. Agrometeorol.,* 3 (1-2): 107-117. https://doi.org/10.54386/jam.v3i1-2.395

Peters-Lidard, C. D., Zion, M. S. and Wood, E. F. (1997). A soil-vegetation-atmosphere transfer scheme for modeling spatially variable water and energy balance processes. *J. Geoph. Res.: Atmos.,* 102(D4): 4303-4324. https://doi.org/10.1029/96JD02948

Rosero, E., Yang, Z. L., Wagener, T., Gulden, L. E., Yatheendradas, S. and Niu, G. Y. (2010). Quantifying parameter sensitivity, interaction, and transferability in hydrologically enhanced versions of the Noah land surface model over transition zones during the warm season. *J. Geoph. Res.: Atmos.,* 115(D3): https://doi.org/10.1029/2009JD012035

Singh, R. P., Oza, S. R., Chaudhari, K. N. and Dadhwal, V. K. (2005). Spatial and temporal patterns of surface soil moisture over India estimated using surface wetness index from SSM/I microwave radiometer. *Intern. J. Remote Sens.,* 26(6): 1269-1276. https://doi.org/10.1080/01431160412331330284

Wang, L., Gao, Z. and Horton, R. (2010). Comparison of six algorithms to determine the soil apparent thermal diffusivity at a site in the Loess Plateau of China. *Soil Sci.,* 175(2): 51-60. https://doi.org/10.5194/hessd-6-2247-2009

Zhao, Y., Si, B., Zhang, Z., Li, M., He, H. and Hill, R. L. (2019). A new thermal conductivity model for sandy and peat soils. *Agric. Forest Meteorol.,* 274: 95-105. https://doi.org/10.1016/j.agrformet.2019.04.004

Zhu, C. and Lettenmaier, D. P. (2007). Long-term climate and derived surface hydrology and energy flux data for Mexico: 1925-2004. *J. Clim.,* 20(9): 1936-1946. https://doi.org/10.1175/JCLI4086.1

Supplementary material

Table ST1: Instrument details on the micrometeorological tower at Ranchi

Sr. No.	Types of observation	Optical Sensor/ Model	Level	Accuracy/Response time/Unit/frequency
1	Wind Speed	05106, 05106C	1, 2, 4, 8, 16 and 32 m	Accuracy: ±0.3 m/s (±0.6 m/s)
2	Air Temperature	HMP45C-L (1000 PRT, IEC 751 1/3 Class B)	1, 2, 4, 8, 16 and 32 mts	Accuracy: ±0.2°C
3	Relative Humidity	HMP45C-L (HUMICAP@180)	1, 2, 4, 8, 16 and 32 m	Accuracy: ±2% RH (0 to 90% RH) ±3% RH (90 to 100% RH)
4	Radiation/ Net Radiation	CNR1 Net Radiometer	2.5 m	Expected accuracy of the temperature measurement: ± 2 K, under non-stable conditions with solar heating or heating by using the heating resistor, Operating temperature: -40°C to 70°C, Expected Accuracy for daily sums: ±10%
5	Radiation/ Short wave (SW)	CM3	2.5 m	Expected Accuracy for daily sums: ±10%,
6	Radiation (Long-wave)	CG3	2.5 m	Accuracy for daily sums: ±10%
7	Soil Heat flux	HFT3 SOIL HEAT FLUX PLATE	2.5, 5.0 cm depth	Accuracy: better than ±5% of reading
8	Soil moisture	CS616 and CS625 Water Content Reflect meters	5, 15 and 30 cm below from the ground surface	Electrical Specification: Output: CS616: ± 0.7-volt square wave with frequency dependent on water content, CS625: 0- 3.3 V square wave with frequency dependent on water content, Resolution: CS616 and CS625 is better than 0.1% volumetric water content.
9	Soil Temperature	107B	Surface, 5, 10, 20, 40 and 100 cm depth	Accuracy: ±0.4°C over the Range of -24^{0}C to 48^{0}C and ± 0.9°C over the range of -38°C to 53°C
10	Rainfall	TE525MM Tipping Bucket Rain Gage	30 cm above the ground surface	Accuracy: Up to 1 in./hr: ± 1%,1 to 2 in./hr: + 0, -3%,2 to 3 in./hr: + 0, -5%

Table ST2: Land-surface parameters prescribed in the model

Description	Parameter	Value	Units
Momentum roughness	Zom	0.1	m
Thermal roughness	Zoh	0.01	m
Minimum canopy resistance	rcmin	13.3	s m –1
Soil porosity	sat	0.41	m 3 m –3
Field capacity	fc	0.25	m 3 m –3
Wilting point	wilt	0.07	m 3 m –3

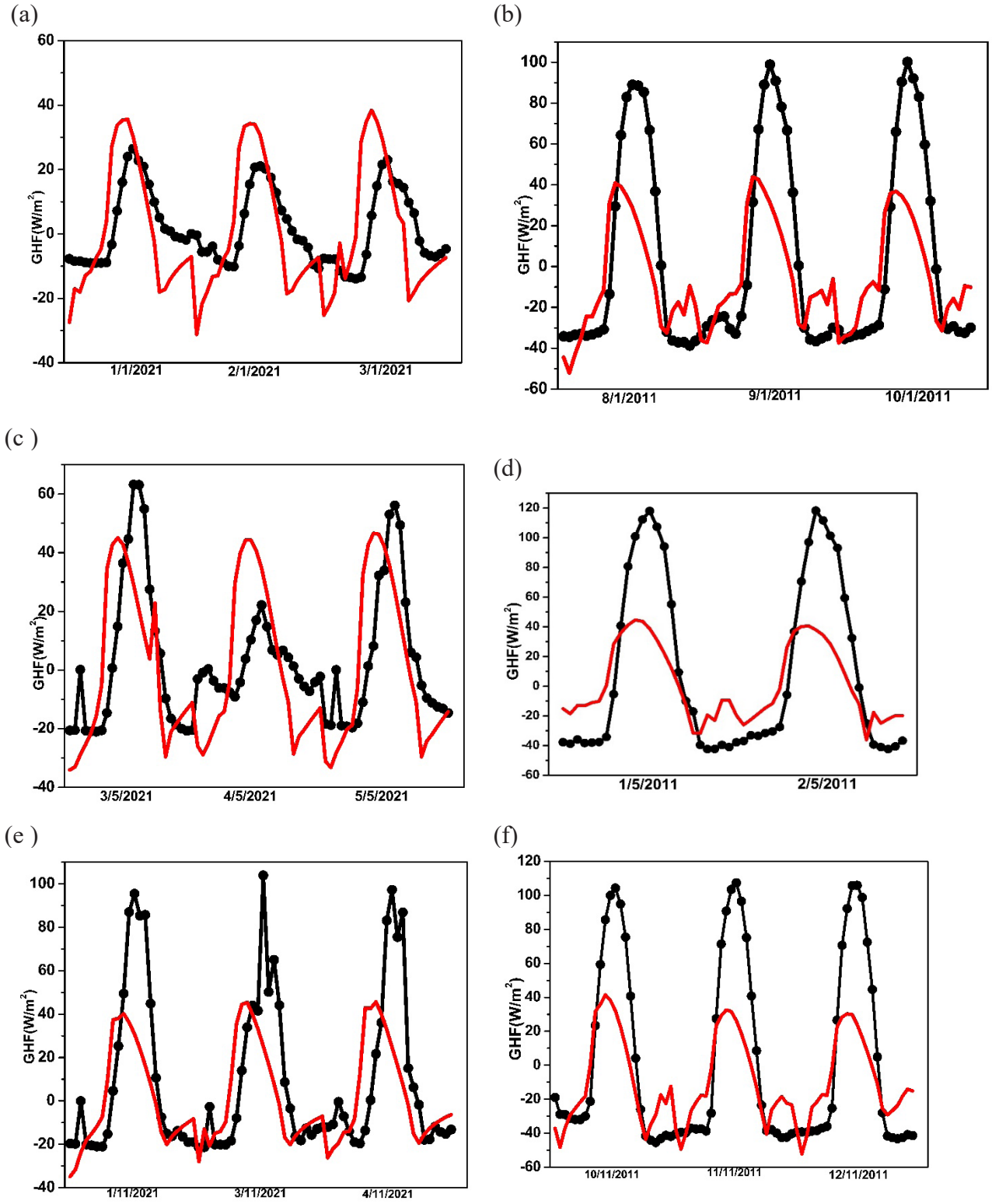

Fig.S1: Diurnal variation of ground heat flux (GHF) in Wm^{-2} at Pune (left column) and at Ranchi (right column) during winter (Jan), Summer (May) and post-monsoon (Nov)